AGU ADVANCING EARTH AND SPACE SCIENCES

Water Resources Research

RESEARCH ARTICLE
10.1029/2024WR037486

Long-Term Performance on Drought Mitigation of Soil Slope Through Bio-Approach of MICP: Evidence and Insight from Both Field and Laboratory Tests

Xin-Lun Ji[1], Chao-Sheng Tang[1], Xiao-Hua Pan[1], Zhao-Lin Cai[1], Bo Liu[2], and Dian-Long Wang[1]

[1]School of Earth Sciences and Engineering, Nanjing University, Nanjing, China, [2]School of Civil and Environmental Engineering, Nanyang Technological University, Nanyang, Singapore

Key Points:

- The eco-friendly technique-microbial induced carbonate precipitation (MICP) performs the time-dependence on long-term drought mitigation
- MICP technique exhibits a remarkable evaporation reduction capacity which is attributed to the presence of soluble salts and hard crust
- This study brings new insights into drought mitigation through a bio-approach and shows the potential for in-situ practice

Correspondence to:

C.-S. Tang and X.-H. Pan,
tangchaosheng@nju.edu.cn;
panxiaohua@nju.edu.cn

Citation:

Ji, X.-L., Tang, C.-S., Pan, X.-H., Cai, Z.-L., Liu, B., & Wang, D.-L. (2024). Long-term performance on drought mitigation of soil slope through bio-approach of MICP: Evidence and Insight from Both Field and Laboratory Tests. *Water Resources Research*, *60*, e2024WR037486. https://doi.org/10.1029/2024WR037486

Received 9 MAR 2024
Accepted 14 JUN 2024

Author Contributions:

Conceptualization: Xin-Lun Ji, Chao-Sheng Tang
Data curation: Xin-Lun Ji
Formal analysis: Xin-Lun Ji, Zhao-Lin Cai
Funding acquisition: Chao-Sheng Tang
Investigation: Xin-Lun Ji, Zhao-Lin Cai, Bo Liu, Dian-Long Wang
Methodology: Xin-Lun Ji, Chao-Sheng Tang, Xiao-Hua Pan, Zhao-Lin Cai
Resources: Xin-Lun Ji, Chao-Sheng Tang
Supervision: Chao-Sheng Tang, Xiao-Hua Pan
Validation: Xin-Lun Ji
Visualization: Xin-Lun Ji
Writing – original draft: Xin-Lun Ji
Writing – review & editing: Xin-Lun Ji, Chao-Sheng Tang, Xiao-Hua Pan

Abstract Drought is a serious global environmental issue that causes water resource scarcity and threatens agriculture and food supplements. This study aims to investigate the long-term performance of an eco-friendly technique-microbial induced carbonate precipitation (MICP) on drought mitigation at field and laboratory scales. Seven in-situ slopes treated with different MICP rounds and cementation solution concentrations were subjected to 16-month weathering. Tests were conducted to evaluate the evaporation characteristics, water retention capacity, and $CaCO_3$ distribution. Laboratory soil samples were further prepared to provide evidence related to underlying weathering mechanisms. The results show that MICP has a time-dependent performance on drought mitigation. After MICP treatment, soil performs a remarkable evaporation suppression ability and the evaporation rate can decrease by 50%. This is attributed to the soluble salts which increase soil water retention capability and dense hard crust which inhibits water vapor migration into the atmosphere. However, the soluble salts and crust are sensitive to weathering thus leading to degradation of MICP. Suffering 16-month weathering, the MICP-induced $CaCO_3$ decreases by more than 60%. The evaporation rate of soil increases with MICP rounds and cementation solution concentrations and can reach nearly two times of untreated soil. MICP-treated field soil exhibits weaker water retention capacity than untreated soil because MICP alters soil microstructure which expands macropores and decreases volume of micropores. Connected macropores act as favorable evaporation channels and accelerate evaporation. To ensure MICP long-term effects, periodical treatments are necessary. The most effective MICP treatment scheme is four to six treatment rounds and 1.0 M cementation solution.

1. Introduction

Drought is considered one of the world's most serious natural disasters (Vicente-Serrano et al., 2020), primarily as a consequence of a decrease in regional precipitation and an increase in evapotranspiration. In recent decades, driven by the intensification of climate change, droughts set in more frequently, become more severe and last longer around the globe (Cook et al., 2015; Naumann et al., 2021; Samaniego et al., 2018), and seriously impacts on ecological, agricultural, and economical sectors (Chiang et al., 2021; Deng et al., 2021). 41% of the global land surface is experiencing drought and it is estimated about 55 million people worldwide every year are affected by problems of food shortage, water scarcity, and deteriorating living conditions (Schumacher et al., 2022; Solh & van Ginkel, 2014). Extreme drought weather results in the excessive evaporation of water in the soil, leading to low soil moisture, that is, soil drought (Li et al., 2022; Mishra & Singh, 2010). Long-term soil drought can cause a series of environmental problems, including widespread vegetation mortality, reduced terrestrial carbon uptake, and even land degradation, soil salinization, and desertification (Chamberlain et al., 2020; Deng et al., 2021; Li et al., 2022; Middleton, 2018). Moreover, drought-induced soil desiccation cracks can further accelerate the evaporation rate, form preferential rainfall infiltration pathways, degrade soil physical and mechanical properties, and cause quite a few geological disasters such as landslides and debris flow (Morris et al., 1992; Senior, 1981; Song & Cui, 2020; Tang et al., 2010; Tang, Shi, et al., 2011). In light of this backdrop, it is of paramount importance to enhance soil water retention capacity and mitigate excessive soil moisture evaporation to alleviate the detrimental impacts of global soil drought.

In order to suppress excessive soil water evaporation and alleviate drought, various sophisticated physical, chemical, vegetation and microbial measures have been employed. Physical measures commonly implemented in arid and semi-arid regions include gravel mulching, straw mulching, and plastic film, which effectively suppress

evaporation. Gravel mulch reduces the evaporation area and increases surface aerodynamic resistance, thereby slowing down the evaporation rate (Yamanaka et al., 2004; Yuan et al., 2009). Straw mulch and plastic film diminish water exchange between soil and atmosphere, thus maintaining soil moisture (Liang et al., 2002). Chemical soil additives such as super absorbent polymer (SAP), polyvinyl alcohol, and polyacrylamide (PAM) were studied and verified the effectiveness in inhibiting soil moisture evaporation (Li, Zhang, et al., 2019; Xiong et al., 2022; Yang et al., 2014). A certain amount of biochar addition was proved to enhance soil water retention capacity (Lu et al., 2021). From a vegetation perspective, afforestation and artificial oasis construction can effectively suppress soil water evaporation (Liu et al., 2010; Zhang & Walsh, 2007). However, the aforementioned methods have inherent limitations. Surface mulches exhibit poor durability, chemical additives have negative impacts on plant growth and the environment, and cultivating vegetation requires high costs. In recent years, a microbial technique named microbial induced carbonate precipitation (MICP) was successfully applied to suppress soil moisture evaporation and improve soil water retention capacity (Liu et al., 2021).

Microbial induced carbonate precipitation (MICP) is a common natural process, whose byproducts alter the properties of soil and other materials (Ivanov & Chu, 2008). Relying on this green, eco-friendly reaction process, MICP technique has attracted more and more attention in recent years and has been widely utilized in various fields, such as soil strength improvement, liquefaction resistance, erosion control, concrete leakage healing, cultural relic repair and heavy metal contaminant remediation (Achal et al., 2012; Jiang & Soga, 2017; Liu, Yu, et al., 2020; Phillips et al., 2013; Sharma & Satyam, 2021; Whiffin et al., 2007). Among various biomediation approaches, one of the most prevalent MICP techniques is a urea hydrolysis process (DeJong et al., 2010; Tang et al., 2020). During this process, ureolytic bacteria produce large amounts of urease through metabolism (Lai et al., 2021; Yang et al., 2022). Catalyzed by the urease, the urea is hydrolyzed and produces ammonium and carbonate ions. The carbonate ions combine with the introduced calcium ions and then generate calcium carbonate ($CaCO_3$) crystals which precipitate throughout the soil matrix while treating soil (Cheng & Cord-Ruwisch, 2012; He et al., 2018; Li, Wang, et al., 2019; Xiao et al., 2022). Liu et al. (2021) treated clayey soil with MICP method and conducted a series of laboratory tests to investigate the MICP treatment effect on evaporation characteristics and microscale behaviors of soil. Experimental results reveal that the MICP technique can improve soil water retention capacity and strengthen inter-particle bonding. The precipitated $CaCO_3$ crystals fill the soil pores which results in a reduction in pore volume and subsequently increase the soil matric suction. In addition, residual soluble salts within soil pores after the MICP process contribute to increased osmotic suction. Consequently, the MICP-treated soil exhibits an enhanced water retention capacity due to the elevated suction. The accumulation of $CaCO_3$ precipitation on the soil surface forms a dense hard crust which suppresses the migration of water vapor into the atmosphere. Moreover, the MICP technique effectively remediates the cracking behavior of clayey soil (Liu, Zhu, et al., 2020; Vail et al., 2020) and significantly reduces the evaporation surface area of soil, thereby further suppressing water evaporation. Though the effects of MICP technique on water evaporation suppression, water retention capacity improvement, and drought mitigation of clayey soil have been verified by lab-scale experiments, the application of the technique at field scale and its long-term performance under climate changes have not been reported.

The objective of the study is to investigate the feasibility, efficiency and durability of applying MICP technique to soil slope drought mitigation. A series of field-scale slope tests treated with different MICP methods were conducted and the evaporation characteristics of the slope were tested after 16 months. This is the first attempt to apply the MICP technique to reduce water evaporation of soil at field-scale tests withstanding long-term climate changes. In order to reveal the mechanisms of MICP technique for soil moisture retention, a series of laboratory tests were conducted including evaporation tests, suction measurement, and mercury intrusion porosimetry (MIP) test. The long-term effects of MICP technique and its mechanism on soil moisture retention were discussed.

2. Materials and Methods

2.1. Soil

The soil tested in this study was Xiashu soil, which is widely distributed in the middle and lower reaches of the Yangtze River. This typical soil is commonly utilized for crop cultivation, vegetation growth and numerous civil engineering projects. According to the USCS classification (ASTM, 2011), the soil can be classified as lean clay

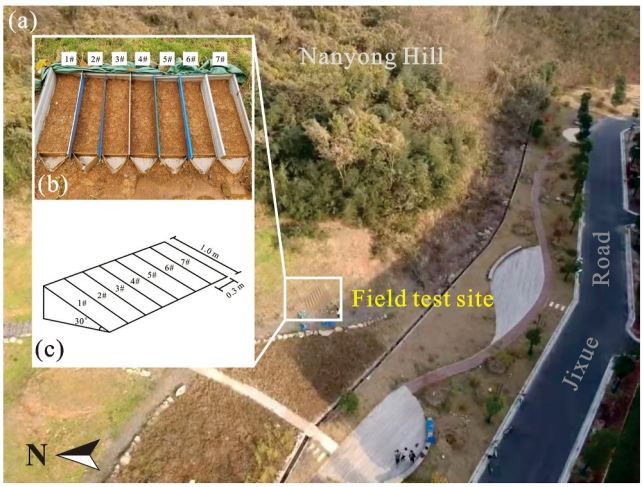

Figure 1. (a) Locations of the field test site, (b) picture, and (c) schematic diagram of test slope.

(CL). Based on the previous study, the majority of clay minerals in this soil are illite-smectite interstratified minerals, illite, and kaolinite.

2.2. Bacteria Suspension and Cementation Solution

The ureolytic bacteria used in this study were *Sporosarcina pasteurii* (ATCC 11859), a kind of widely prevalent bacteria in the natural environment, which has strong proliferation capacity, is easy to cultivate, and exhibits high urease activity (DeJong et al., 2010). First, the source bacteria were inoculated into the sterilized solid ammonium yeast extract (NH_4-YE) medium (10 g/L ammonium sulfate ($(NH_4)_2SO_4$), 20 g/L yeast extract, 15.73 g/L Tris buffer, and 20 g/L agar) with dilution plate streaking method to purify. After cultivation at 30°C for 24 hr, a few single colonies were picked out and subsequently transferred to the sterilized liquid medium (20 g/L yeast extract, 10 g/L ammonium sulfate ($(NH_4)_2SO_4$), and 15.73 g/L Tris buffer). The prepared bacteria suspension (BS) was then cultured in a shaking incubator (at 30°C and 200 rpm) for 24 hr. After cultivation, the measured optical density (OD_{600}) of the BS was 1.0 ± 0.2 (Okwadha & Li, 2010; Whiffin et al., 2007). Subsequently, 5 mL BS was extracted to assess its urease activity, resulting in a measured value of 7.5 mM urea hydrolyzed per minute.

The cementation solution (CS) can provide a calcium source for microbial mineralization reactions (Tang et al., 2023). In this study, two concentration levels (0.5 and 1.0 M) of CS were employed to treat soil. The 0.5 M CS was composed of 0.5 mol/L urea, 0.5 mol/L calcium chloride ($CaCl_2$), and 3.0 g/L Nutrient Broth. And 1.0 M CS was composed of 1.0 mol/L urea, 1.0 mol/L calcium chloride ($CaCl_2$), and the same concentration of Nutrient Broth.

2.3. Field Treatment and In-Situ Samples Test Method

2.3.1. Test Site Condition and MICP Treatment Scheme

Figure 1a shows the locations of the field test site. The test site (118°57′15″E, 32°7′20″N) is seated in Nanjing, Jiangsu Province, China. The test site is part of a clayey artificial slope and shows a width of 2.1 m, a height of 0.5 m, a gradient of 30°, and a slope surface length of about 1.0 m, as shown in the schematic view of the slope in Figure 1c. The slope had suffered from long-time weathering, resulting in soil erosion, gully development, and vegetation destruction, which seriously affected the stability and ecological environment of the slope. Figure 1b shows the picture of the slope before MICP treatment. The previous study (Liu, Zhu, et al., 2020) shows the surface soil of the slope is under a loose state after long-term weathering, with a large number of macro-pores and micro-cracks observed in the soil. The pore size distribution curves demonstrate the soil is suitable for MICP treatment.

Before MICP treatment, the ruderal weeds on the test slope were cleared and the slope surface was leveled. The test slope was evenly divided into seven parts and numbered 1# to 7#. Iron plates were used as barriers between each part, including the top of the test slope, to prevent the accumulation of eroded soil from the slope above, thereby avoiding any impact on the observation results.Spraying method (Cheng et al., 2021) was adopted for MICP treatment in this study. Each round of MICP treatment consisted of two steps. First, 2 L of BS was uniformly sprayed on the slope surface. Subsequently, 2 L of CS was uniformly sprayed on the slope surface. A six-hour interval between the two steps was necessary to ensure sufficient infiltration of the BS and bacteria colonization. Each slope was treated with different MICP treatment schemes except Slope 1#. Slope 2# - 4# were treated by MICP with 0.5 M CS for 2, 4, and 6 rounds respectively, meanwhile, Slope 5# - 7# were treated by MICP with 1.0 M CS for 2, 4, and 6 rounds respectively. The slope number and MICP treatment schemes are exhibited in Table 1. To reveal the long-term performance of the water retention capacity of the MICP-treated soil slope, the test slope was subjected to 16 months of weathering and then sampled for the following tests. Figure 2 shows the pictures of the slopes after MICP treatment and 16 months of weathering, respectively.

Table 1
Numbers and MICP Treatment Schemes for Field Test Slopes

Slope no.	Treatment round	Treatment method	Concentration of CS
1#	/	/	/
2#	2	Two-steps MICP treatment	0.5 M
3#	4	Two-steps MICP treatment	0.5 M
4#	6	Two-steps MICP treatment	0.5 M
5#	2	Two-steps MICP treatment	1.0 M
6#	4	Two-steps MICP treatment	1.0 M
7#	6	Two-steps MICP treatment	1.0 M

2.3.2. Evaporation Test

MICP treatment inevitably suffers an inherent non-uniformity effect when treating clayey soil slopes for the flow of treatment solution. Hence, the evaporation test samples were collected from the upper, middle, and lower sections of each slope, respectively. Sampling steel rings were used to obtain the evaporation test samples, therefore the evaporation characteristics of the top 2 cm depth soil were tested. Figure 3a displays the specific sampling locations of tests.

Figure 2. Pictures of test slopes after MICP treatment and after 16-month weathering.

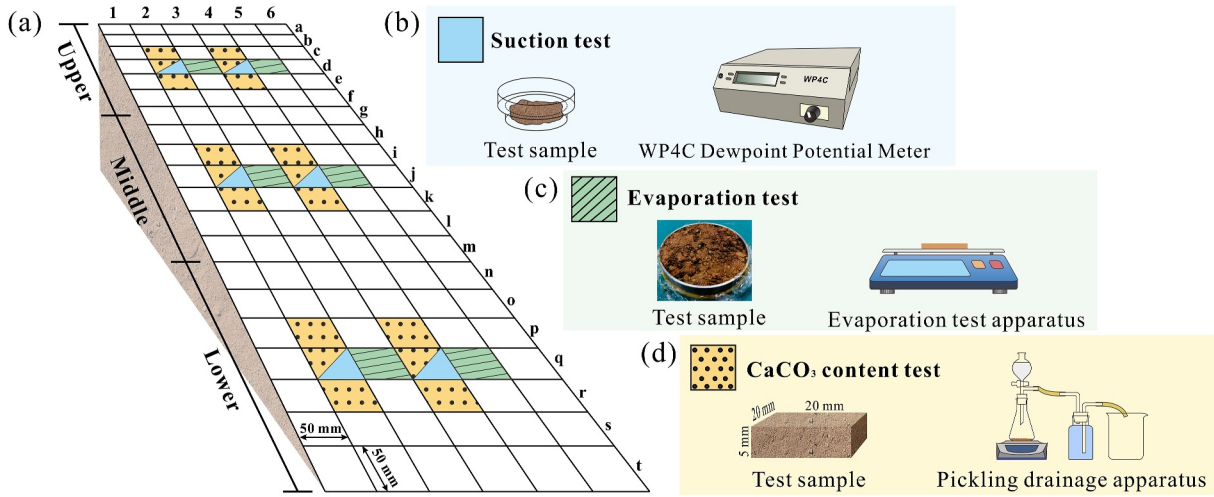

Figure 3. Sampling locations and test apparatus for suction test, evaporation test, and calcium carbonate content test.

Before the laboratory evaporation test, samples were covered with grease at the sidewall and bottom and then securely wrapped with cling film like Figure 3b, exposing only the upper surface as the evaporation surface. Subsequently, samples were saturated and then allowed to dry at a stable room temperature of 30 ± 2°C and relative humidity of 50 ± 5%. Each sample was weighted every 2 hrs to calculate the actual evaporation rate (E_a). A pure water sample was subjected to the same environmental conditions to serve as a reference for measuring the potential evaporation rate (E_p). This parameter represented the maximum rate at which water evaporates in a free state without soil (An et al., 2018). The ratio of E_a to E_p can eliminate the influence of environmental fluctuations (temperature and humidity) on the evaporation rate and can be calculated by Equation 1.

$$E_a/E_p = \frac{(W_{s,i+1} - W_{s,i})/t}{(W_{w,i+1} - W_{w,i})/t}, i \geq 1 \quad (1)$$

where $W_{s,i}$ and $W_{w,i}$ are soil sample weight and pure water sample weight from the ith measurement, respectively, and t is the time interval between two consecutive measurements.

2.3.3. Soil Water Characteristic Curve Measurement

In order to investigate the retention capacity of the slope surface soil, soil clods with about 20 mm diameter and 5 mm thickness were extracted from the upper, middle, and lower sections of the slope. The sampling locations are shown in Figure 3a. WP4C Dewpoint Potential Meter was utilized for suction measurement (Figure 3c). Ultimately, a soil-water characteristic curve (Fredlund et al., 2002) of each soil clod measured during the drying process was obtained.

2.3.4. Calcium Carbonate Content Test

Calcium carbonate content is a criterion for evaluating the effect of MICP treatment. Pickling drainage method (Tang et al., 2023) was adopted to measure the calcium carbonate content of the slope surface (depth of 0–20 mm) soil. Each sample was about 5 g of soil collected from the upper, middle, and lower sections of each slope, respectively. The sampling locations are shown in Figure 3a. The soil was first oven-dried and weighted as M. Subsequently, the sample was dissolved in 100 mL hydrochloric acid solution of 1.0 mol/L. Calcium carbonate in soil reacted with the hydrogen chloride and produced carbon dioxide which drained the same volume of water. The water was collected, the volume of which was recorded as V. The calcium carbonate content of soil can be calculated by Equation 2.

Table 2
Numbers and MICP Treatment Methods of Laboratory Test Samples

Sample no.	Treatment method	Concentration of CS during MICP	MICP treatment round
M0	-	-	-
M0.5-2	MICP	0.5 M	2
M0.5-4	MICP	0.5 M	4
M0.5-6	MICP	0.5 M	6
M1.0-2	MICP	1.0 M	2
M1.0-4	MICP	1.0 M	4
M1.0-6	MICP	1.0 M	6
W0	MICP-Wash salts	-	-
W0.5-2	MICP-Wash salts	0.5 M	2
W0.5-4	MICP-Wash salts	0.5 M	4
W0.5-6	MICP -Wash salts	0.5 M	6
W1.0-2	MICP-Wash salts	1.0 M	2
W1.0-4	MICP -Wash salts	1.0 M	4
W1.0-6	MICP -Wash salts	1.0 M	6
R0	MICP -Wash salts -Remove crust	-	-
R0.5-2	MICP -Wash salts -Remove crust	0.5 M	2
R0.5-4	MICP -Wash salts -Remove crust	0.5 M	4
R0.5-6	MICP -Wash salts -Remove crust	0.5 M	6
R1.0-2	MICP -Wash salts -Remove crust	1.0 M	2
R1.0-4	MICP -Wash salts -Remove crust	1.0 M	4
R1.0-6	MICP -Wash salts -Remove crust	1.0 M	6

$$CaCO_3(\%) = \frac{100 \cdot V}{24.5 \cdot M} \times 100\% \quad (2)$$

2.4. Laboratory Samples Test Method

In order to explore the reasons for the variation of the suppression effect of MICP treatment on the evaporation rate of slope under long-term climate change, a supplementary lab-scale test was carried out. Nine soil samples were extracted with sampling steel rings adjacent to the test site mentioned above. Subsequently, these samples were treated with the same MICP method as the field test. Table 2 shows the numbers and MICP treatment methods of laboratory test samples.

Figure 4a shows the schematic drawing of the laboratory test procedure and Figure 4b shows the pictures of the initial sample, MICP-treated samples, and sample with salts removal. The samples were subjected to three evaporation tests, after MICP treatment, soluble salts washing off, and hard crust removal, respectively. The evaporation tests were conducted following the same procedure as described in Section 2.3.2. The process of washing off soluble salts involved percolating the samples with deionized water until the conductivity of the filtered liquid approached zero. To eliminate the hard crusts induced by calcium carbonate precipitation completely, a 0.5 cm layer of surface soil was removed from each sample. The samples without MICP treatment (G0) were subjected to evaporation tests after water spraying, salt washing, and removal of the surface soil. Simultaneously, after each evaporation test, a 0.5 cm thickness of soil was extracted from each sample group for suction testing and mercury intrusion porosimetry (MIP) to analyze the soil water characteristic curve and microstructures.

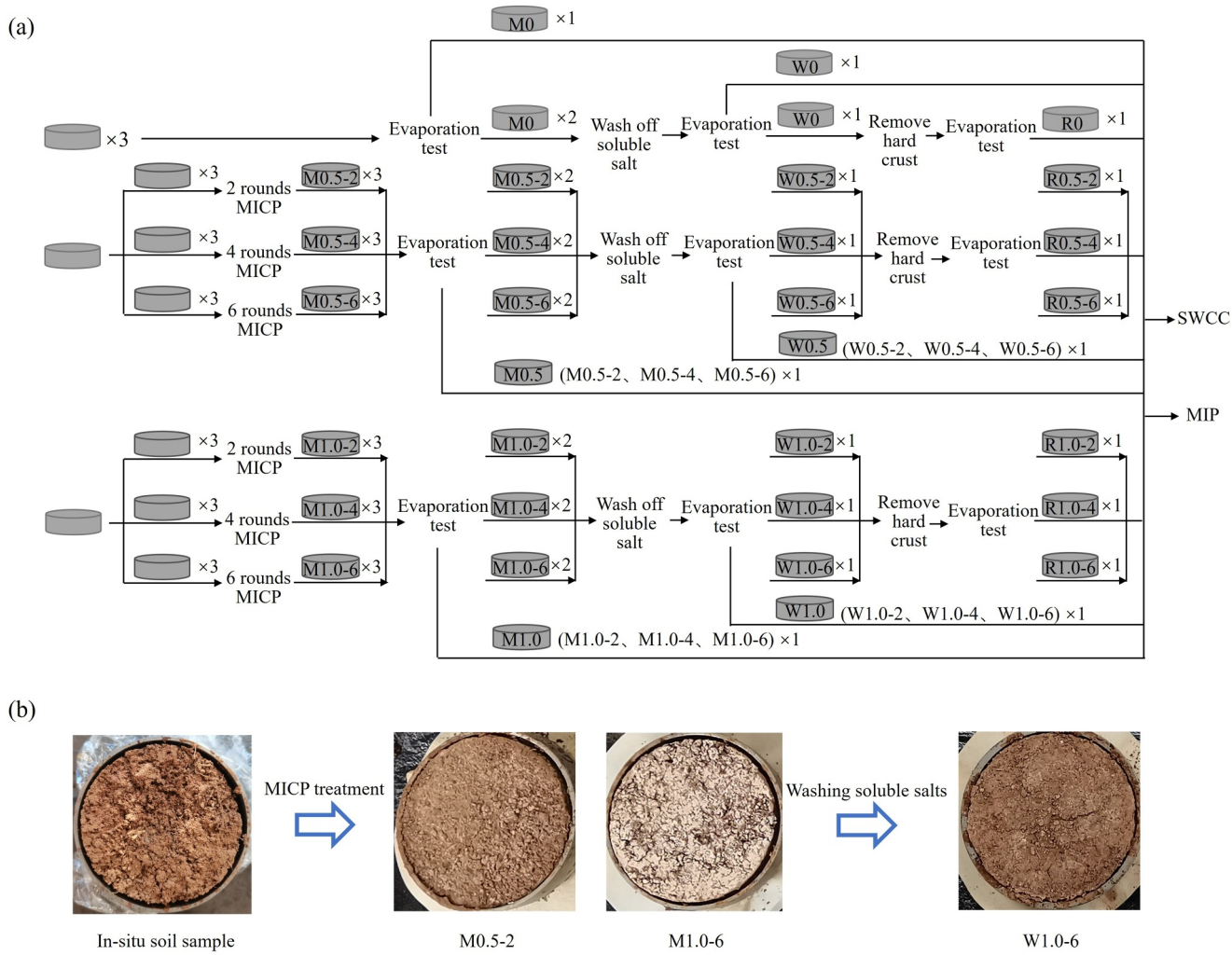

Figure 4. (a) Schematic drawing of the laboratory test procedure and (b) pictures of the initial sample, MICP-treated samples, and sample with salts removal.

3. Results

3.1. In-Situ Samples

3.1.1. Evaporation Process

Figure 5 illustrates the variations of the ratio of actual and potential evaporation (Ea/Ep) versus time of the test Slopes 1# to 7#. Due to the similarity in the evaporation behavior of samples obtained from the upper, middle, and lower sections of the slope, the evaporation curves of the samples of lower sections are presented in Figure 5 for analysis. In general, after the long-term effect of climate, the evaporation rate of MICP-treated soil was larger than that of untreated soil, indicating that the MICP induced drought resistance effect weakened.

The evaporation processes of all samples can be divided into three stages (Tang, Cui, et al., 2011; Wilson et al., 1994): constant rate stage (I), falling rate stage (II), and residual stage (III). For instance, on Slope 1#, the three stages corresponded to 0–42 (t_1) hrs, 42–92 (t_1') hrs, and 92–177 hr of the evaporation process, respectively. In the constant rate stage, the value of Ea/Ep of each sample exceeded 1.0. This is due to the fact that the rough surface of the undisturbed soil led to an increased evaporation surface area, whereas the calculations were based on the surface area of the steel ring. From Figure 5, it can be seen that the evaporation rates of MICP-treated samples prevailed higher than those of untreated soil. With the increase of MICP treatment rounds, evaporation rates of samples increased and the during time of constant rate stage prolongs. The duration of samples from Slopes 2#, 3#, 4# and 5#, 6#, 7# were 41.6 hr, 38.0 hr, 18.0 hr and 38.8 hr, 24.0 hr, 14.5 hr, respectively. The

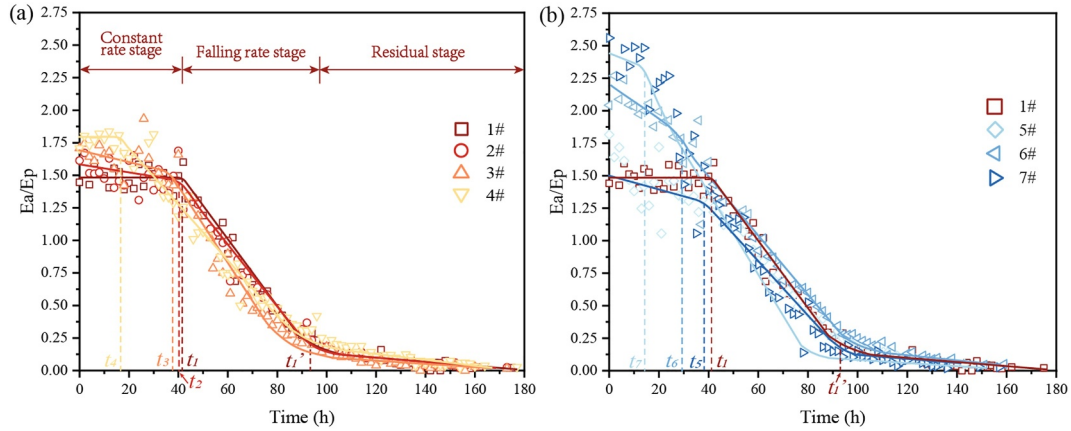

Figure 5. Variations of the ratio of actual and potential evaporation (Ea/Ep) versus time of the test slopes (a) 1#, 2#, 3#, 4#, and (b) 1#, 5#, 6#, 7#.

samples treated with higher concentrations of CS displayed much larger evaporation rates than samples treated with lower concentrations of CS. After MICP treatment, evaporation rates of samples within the constant rate stage no longer maintained a constant value but gradually decreased, though the decrease was less significant than the deceleration in the falling rate stage. This phenomenon was more evident when the soil was treated with a higher concentration of CS and more rounds of MICP treatment.

During the falling rate stage, the evaporation rate of MICP-treated soil was generally lower than that of untreated soil. The evaporation rate of MICP-treated soil decreased rapidly during the falling rate stage, with a greater magnitude of decrease than that observed in the untreated soil. Furthermore, as the concentration of CS and MICP treatment rounds increased, the samples exhibited a longer duration of the falling rate stage.

With regard to the residual stage, all samples prevalently entered this phase simultaneously, typically around 80–90 hr, and the evaporation rate of each sample consistently remained at a low level.

Figure 6 shows the variations in the ratio of actual and potential evaporation (Ea/Ep) versus the time of samples extracted at the upper, middle, and lower sections of Slope 7#. As can be seen in Figure 6, there were variations in the effectiveness of the MICP treatment across the upper, middle, and lower sections of the slope, indicating an uneven performance within the test site. During the constant rate stage, the evaporation rate of soil increased progressively from the upper to the lower sections of the slope, while the duration of the constant rate stage became shorter. In the falling rate stage, the duration of the falling rate stage of the samples increased from the upper to the lower sections of the slope. The evaporation rate of the lower section samples during the falling rate stage was significantly lower than upward soil.

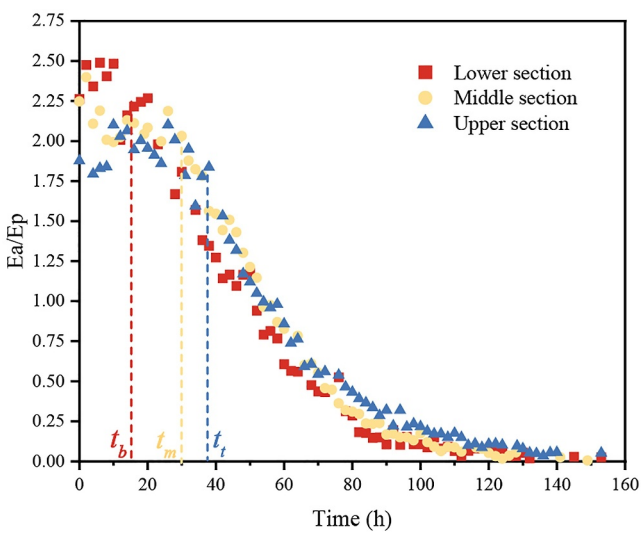

Figure 6. Variations of the ratio of actual and potential evaporation (Ea/Ep) versus time of 7# slope at upper, middle, and lower sections.

3.1.2. Soil Water Retention Capacity

Figure 7 presents the soil water characteristic curves during the drying process for samples collected from the upper, middle, and lower sections of each slope site. The Van Genuchten (VG) equation was employed for fitting the data (van Genuchten, 1980). Figure 7 reveals variations in the water retention capacity among the upper, middle, and lower sections of the slope, indicating non-uniformity resulting from both the MICP treatment and long-term weathering processes. The water retention capacity of the samples in the middle and lower sections of each slope exhibited relative similarity, whereas notable differences were observed among samples in the upper section. Generally, the samples in the upper section exhibited higher suction at identical water content, signifying a stronger water retention capacity compared to the middle and lower sections of the slopes. This observation aligned with the results of the evaporation tests (Figure 6), which

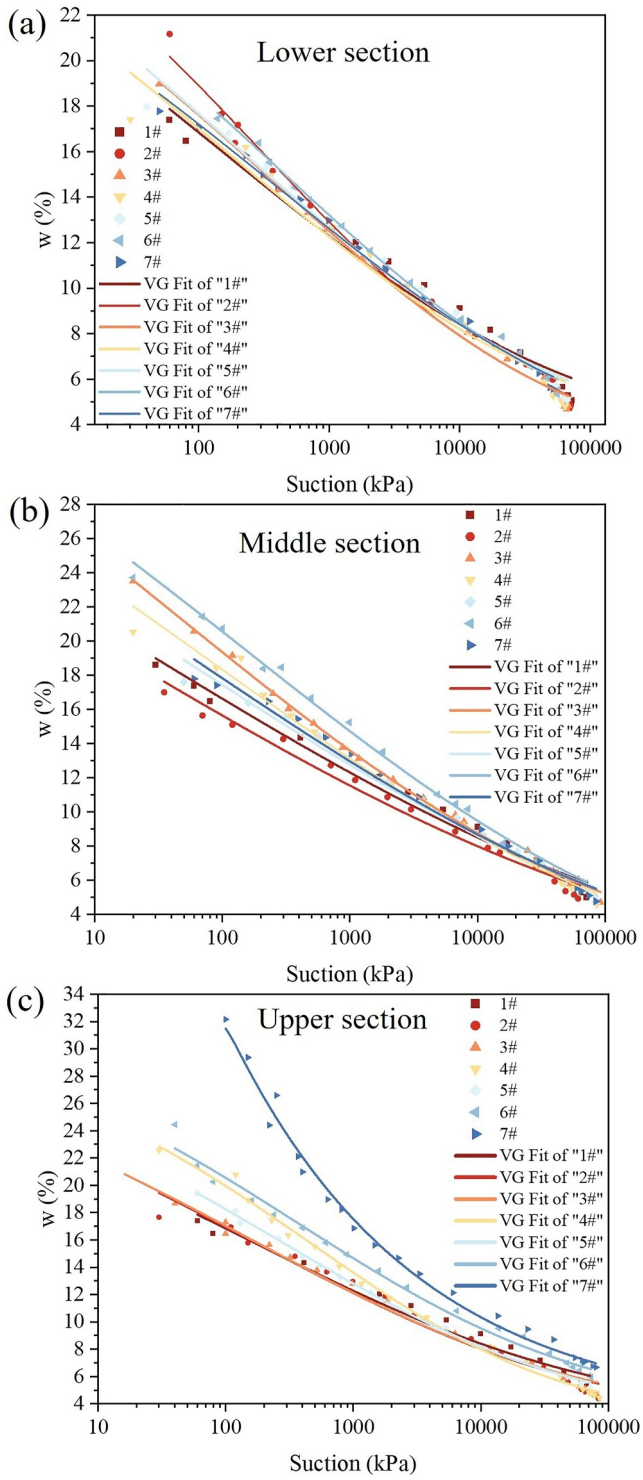

Figure 7. Soil water characteristic curves of soil sampled at (a) lower, (b) middle and (c) upper sections of slopes 1# to 7#.

demonstrated that soils with higher water retention capacity (i.e., upper-section soils) exhibited slower evaporation rates.

When considering the upper soil of different slopes (Figure 7c), under identical water content, the untreated soil (Slope 1#) exhibited lower suction compared to the MICP-treated soils (Slopes 2#-7#), indicating that the MICP-treated soil in the upper sections of the slopes maintained a certain level of water retention capacity even after undergoing long-term weathering. Furthermore, an increasing trend in the water retention capacity of the soil was observed as the rounds of MICP treatment and the concentration of CS increase. The suction of the soil sample collected from Slope 7# can reached 1,010 kPa at a water content of 16.5%, which was 12.6 times the suction of the sample from Slope 1# at the same water content.

3.1.3. Calcium Carbonate Content

Figure 8a depicts the calcium carbonate content of the surface soil at different locations (upper, middle, and lower sections) of the MICP-treated slopes (Slopes 2#-7#) after MICP treatment and 16 months of weathering. The natural Xiashu soil slope has a calcium carbonate content of approximately 0.2% as measured. From Figure 8a, it can be observed that the calcium carbonate content of soil significantly increased after MICP treatment. The calcium carbonate content in the lower section of Slope 7# (subjected to 6 rounds of MICP treatment with 1.0 M CS) was approximately 18 times higher than that of the untreated soil. With an increase in both MICP treatment rounds and the concentration of CS, the yield of calcium carbonate during the MICP process increased. This can be attributed to the larger concentration of CS which provided more calcium sources for the MICP reaction, and multiple treatment rounds which supplied additional bacteria and nutrients, thereby promoting the generation of calcium carbonate.

As shown in Figure 8a, the distribution of calcium carbonate across the upper, middle, and lower sections of the slopes was non-uniform. In general, the calcium carbonate content was higher at the lower section of slopes compared to the middle and upper sections. This disparity became more pronounced with an increasing number of MICP treatment rounds. During MICP treatment, the spraying method was adopted to apply the treatment solution to slopes. A portion of the treatment solution infiltrated into the slope, while another portion flowed downward along the slope surface due to gravity. A greater amount of treatment solution accumulated at the foot of the slope, resulting in an increased production of calcium carbonate precipitation.

Figure 8a simultaneously reveals a substantial decline in the calcium carbonate content of all slopes after 16 months of weathering. Among them, the calcium carbonate content of Slopes 2#, 3#, and 4# (0.5 M CS) at various sections was approximately at the same level as the untreated soil. In contrast, Slopes 5#, 6#, and 7# (1.0 M CS) retained relatively more calcium carbonate, and the conserved quantity of calcium carbonate increased with the increase of MICP treatment round. Slope 7# retained the highest calcium carbonate content, with a calcium carbonate content of 1.3% in the lower section, which was 40% of calcium carbonate after MICP treatment. Slopes 3# and 5# had similar calcium carbonate content after MICP treatment, though Slope 5# retained a conspicuously larger amount of calcium carbonate after long-term weathering. This indicated that for slopes with similar initial MICP treatment effects, the concentration of CS proved more effective in enhancing long-term weathering resistance.

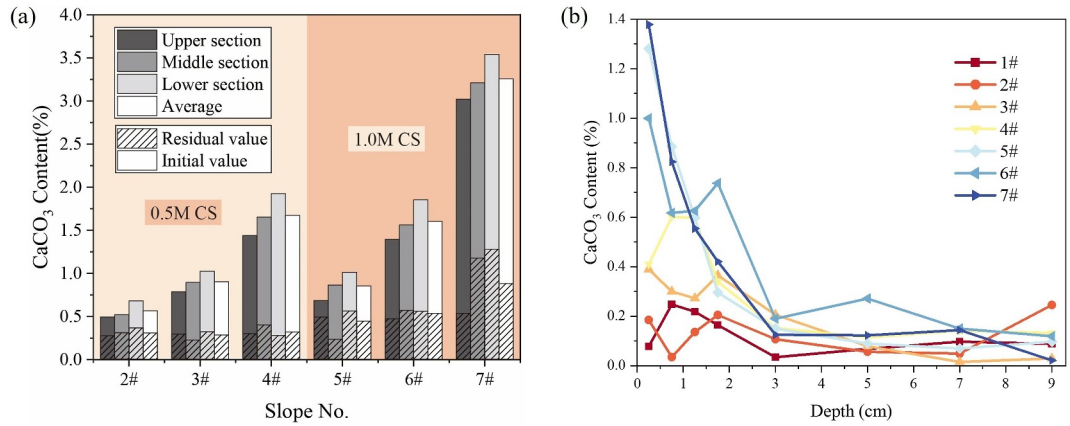

Figure 8. (a) Calcium carbonate content of slopes 2# to 7# after MICP treatment and 16 months of weathering; (b) Variations of calcium carbonate content versus depth of slopes 1# to 7# after 16 months of weathering.

Figure 8b shows the variations of calcium carbonate content versus depth of slopes 1# to 7# after 16 months of weathering. Generally, the calcium carbonate content decreased gradually with increasing depth across all slopes. Within the depth range of 0–3 cm, a sharp reduction in the calcium carbonate content occurred as depth increases. The decreasing trend became more obvious with the increase in MICP treatment rounds and CS concentration. At a depth of 3 cm, the calcium carbonate content at Slope 7# was merely 9% of the surface soil, while for Slope 2#, it was 58%. Within the depth range of 0–3 cm, the influence of MICP treatment rounds and the concentration of CS was apparent, with more treatment rounds and higher CS concentration resulting in a larger amount of calcium carbonate content. Nevertheless, below the depth of 3 cm, the calcium carbonate content of all slopes remained consistently at a low level, fluctuating between 0% and 0.3%. Furthermore, the calcium carbonate content in each slope no longer decreased as depth increases. And the effects of MICP treatment rounds and concentration of CS became negligible.

3.2. Laboratory Samples

3.2.1. Evaporation Process

Figure 9 depicts the variations in the ratio of actual and potential evaporation (Ea/Ep) versus the time of samples after MICP treatment, soluble salts washed off, and hard crust removal. After MICP treatment (Figure 9a), the evaporation rates of samples decreased at the beginning of evaporation process which indicated the constant rate stages of these samples were not conspicuous. Nevertheless, the evaporation process of untreated sample (M0) followed a three-stage pattern. These results were consistent with the study of Liu et al. (2021). Moreover, the evaporation rates performed a significant difference among samples with various MICP treatment methods throughout the whole evaporation process. As MICP treatment rounds and concentration of CS increase, the evaporation rates of samples diminished monotonically, with the lowest value obtained from the soil sample treated with six rounds of MICP using 1.0 M CS (sample M1.0-6). MICP treatment significantly reduced the evaporation rate of soil and inhabited dissipation of moisture, therefore performing remarkable drought resistance.

After the soluble salts (including calcium chloride, ammonium chloride, etc.) washing-off step, the evaporation process of all samples exhibited a three-stage pattern and their evaporation curves largely coincide (Figure 9b). The evaporation rate of untreated soil sample (W0) remained relatively unchanged compared to Figure 9a. The evaporation rate of each MICP-treated sample increased to varying degrees after multiple rounds of salts leaching filtration, eventually reaching a level similar to that of the untreated soil. The increase in the evaporation rate of the sample after salt washing became more pronounced with an increase in the number of MICP treatment rounds and the concentration of CS. These results indicated that soluble salts had a positive effect on reducing the evaporation rate of soil.

Hard crust formed during MICP treatment process acted as an evaporation barrier and effectively reduced the soil moisture loss in lab-scale compacted soil samples (Liu, Zhu, et al., 2020). However, in in-situ undisturbed soil

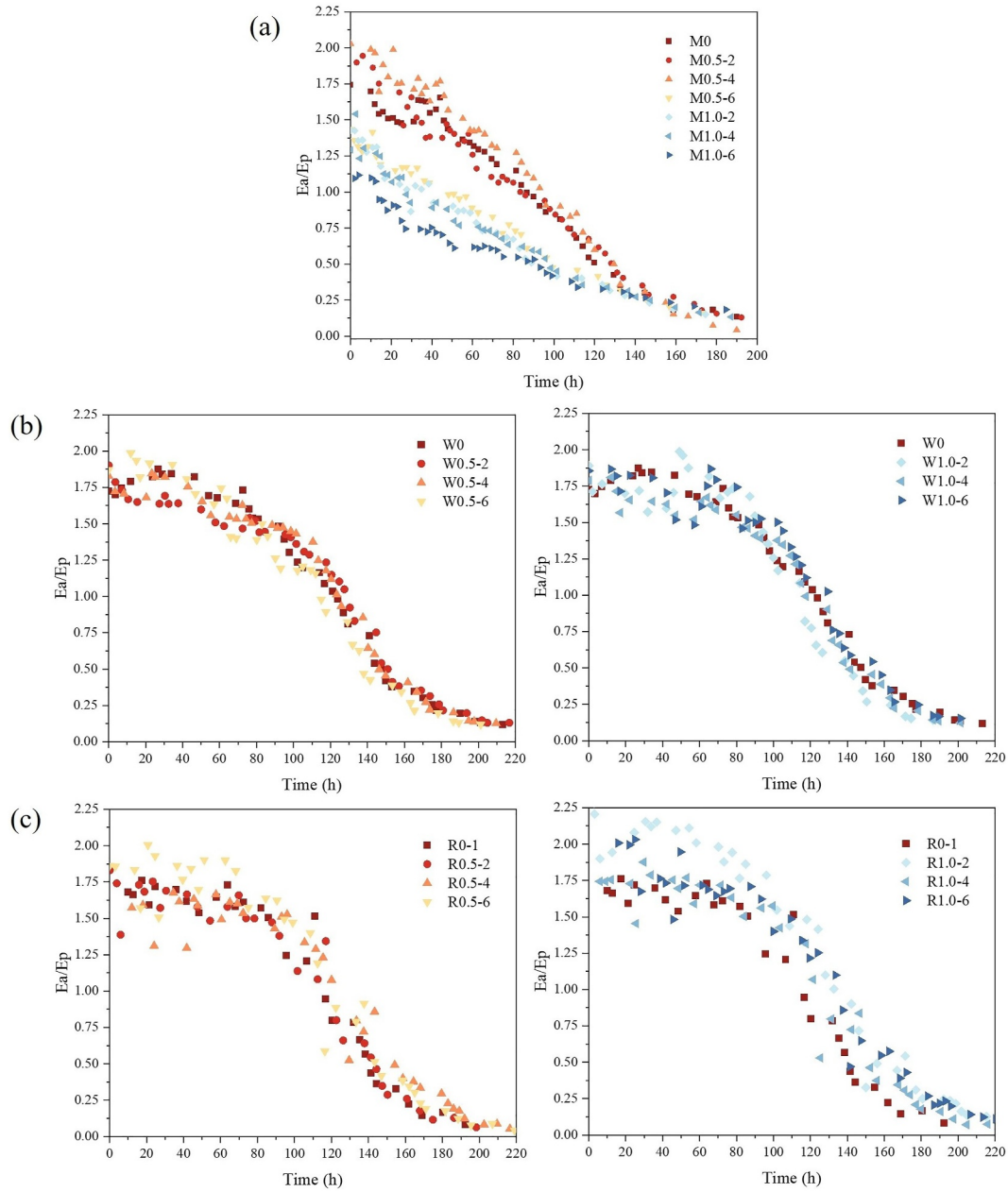

Figure 9. Variations of the ratio of actual and potential evaporation (Ea/Ep) versus time of samples after (a) MICP treatment, (b) soluble salt wash-off, and (c) hard crust removal.

samples, it was challenging to develop an integrated hard crust due to the rough soil sample surface. Moreover, the loose and fragile hard crust was prone to denudation and failure over a long period of weathering and erosion. To determine the practical effect of hard crust on evaporation rate of undisturbed soil, the evaporation processes of the aforementioned samples after hard crust removal were monitored. As shown in Figure 9c, the pattern of each evaporation curve remained relatively consistent compared to Figure 9b. After hard crust removal, the evaporation rates of MICP-treated samples further increased and exceeded those of untreated soil. However, the evaporation rates of MICP-treated samples had a close relationship with the dry density of samples. This correlation arose from the fact that the removal of hard crust exposed numerous large pores and micro-fissures in the soil which promoted evaporation drastically.

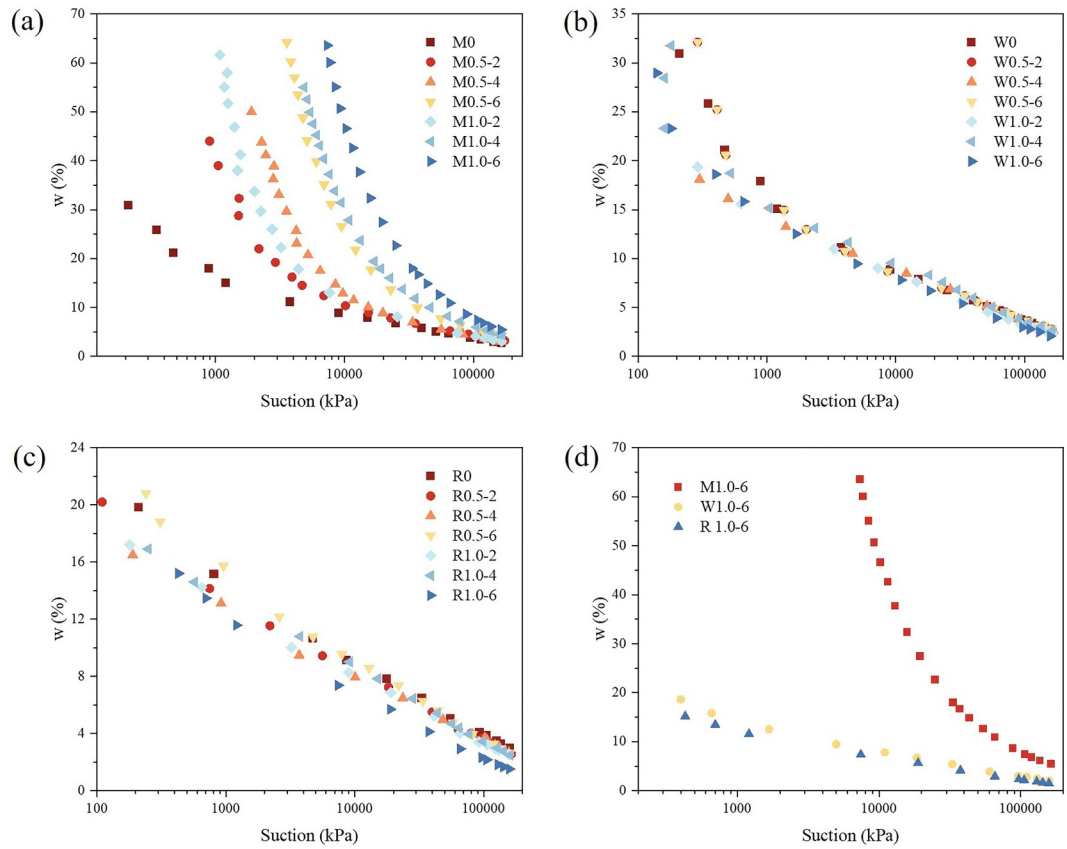

Figure 10. Soil water characteristic curves of all samples after (a) MICP treatment, (b) soluble salt removal, (c) hard crust removal; and (d) soil water characteristic curves of samples M1.0–6, W1.0-6, and R1.0-6.

In conclusion, both the soluble salts and hard crust played important roles in reducing the evaporation rate of the soil.

3.2.2. Soil Water Retention Capacity

Figure 10a–10c show the soil water characteristic curves of samples after MICP treatment, soluble salts washing off, and hard crust removal. After MICP treatment, the soil water characteristic curves among samples were quite different. At equivalent water content, the suctions of MICP-treated soil samples were significantly higher than those of untreated soil (M0), indicating that MICP treatment effectively improved the water retention capacity of soil. With an increase in the number of MICP treatment rounds and CS concentration, the water retention capacity of soil was enhanced. At a water content of 18%, the suction of sample M1.0-6 was 33,350 kPa, nearly 38 times greater than that of sample M0.

As can be seen in Figure 10b, after washing off the soluble salts, the water retention capacities of soil samples subjected to different MICP treatment methods tended to be similar. The suctions of MICP-treated samples decreased apparently and remained at comparable levels to untreated soil. For instance, at a water content of 10%, the suction of sample W1.0-6 exceeded 70000 kPa after MICP treatment, whereas it reduced to 3,500 kPa after washing off the soluble salts, which represented only 5% of the previous value (Figure 10d).

To eliminate the hard crust, a 0.5 cm-thick layer of soil on the sample surface was removed. This procedure did not disrupt the internal microstructures of the soil below the hard crust. As a result, the soil water characteristic curve of soil below the hard crust in each sample did not exhibit significant changes, and the water retention capacity of each sample remained approximately the same (Figure 10c).

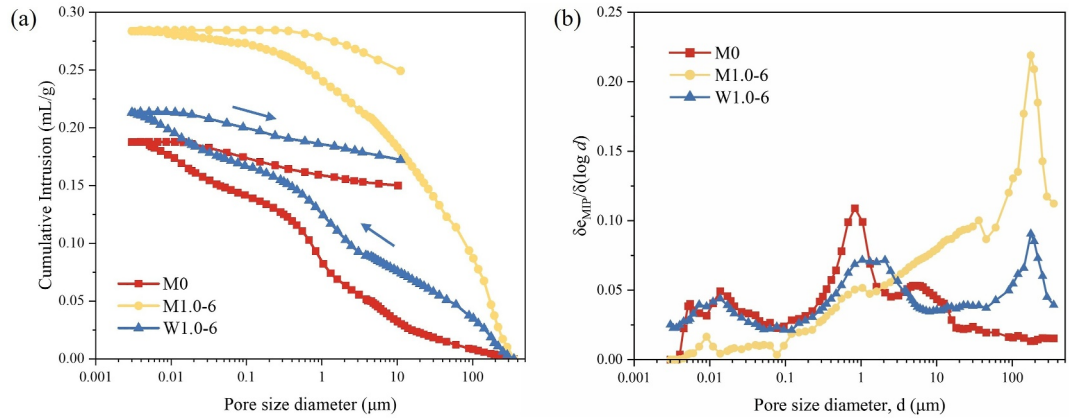

Figure 11. (a) Cumulative mercury intrusion and extrusion curves of samples M0, M1.0–6, W1.0-6; (b) Pore size distribution curves of samples M0, M1.0–6, W1.0-6.

3.2.3. Pores Size Distribution

The MIP results of soil samples M0 (untreated), M1.0-6 (MICP treated), and W1.0-6 (washing off soluble salt) in the laboratory test are shown in Figure 11. Figure 11a illustrates the cumulative mercury intrusion and extrusion pore volume normalized by the sample weight of those samples. Notably, the undisturbed soil sample M0 had the lowest value of total cumulative intrusion pore volume. After MICP treatment, total cumulative intrusion pore volume of the sample M1.0-6 reached the value of 0.285 mL/g, which indicated that MICP treatment resulted in a significantly increased porosity of soil. After washing off the soluble salts, the porosity of soil sample W1.0-6 decreased while still larger than M0. Furthermore, the intrusion curve and extrusion curve of each sample followed different paths. The difference between the intrusion and extrusion cycle was the entrapped or constricted porosity, which accounted for the main reduction in total volume (Romero et al., 1999).

Figure 11b shows the pore size distribution (PSD) curves of soil samples M0, M1.0–6, W1.0-6 in the laboratory test. The ordinate is the pore size density function which is defined as $\delta e_{MIP}/\delta(\log d)$, where d is the entrance pore diameter and e_{MIP} is the porosity obtained by dividing the cumulative mercury volume by the soil particle volume. As can be seen from Figure 11b, sample M0 displayed a relatively uniform pore size distribution and a unimodal feature with dominant pore diameters around 0.8 μm. After MICP treatment, the sample M1.0-6 shifted the size of dominant macropores toward a significantly larger value of around 176 μm and the macropores density of the sample increased conspicuously and accounts for more than 80% of the total cumulative pore volume. Moreover, the volume of micropores decreased significantly due to the soluble salt crystals and organisms filling in pores which were introduced by MICP treatment. After washing off the soluble salt, sample W1.0-6 can be characterized by a clear bimodal distribution but with different dominant pore modes. Sample W1.0-6 displayed the dominant pore diameters around 2 μm (micropores) and 200 μm (macropores), which represented intra-aggregate pores and inter-aggregate pores, respectively (Romero et al., 2011). The size of these two dominant pore diameters was not affected by salt-washing while the total volume of micropores increased and macropores decreased. Comparing the samples M0 and W1.0-6, an apparent change was that the macropores expanded significantly which might be attributed to the shrinkage of sample after drying.

4. Discussion

4.1. Mechanism of MICP Treatment on Soil Evaporation Reduction

The critical issue of soil drought mitigation is suppressing water evaporation from soil and keeping the soil moist. The evaporation process of moisture in soil is influenced by a variety of factors, both exterior and interior (Tang, Cui, et al., 2011). Atmospheric conditions, including vapor pressure, airflow speed, relative humidity and temperature, and solar radiation can significantly change the evaporation rate (Gilliland, 1938; Yamanaka et al., 1997). The interior factors mainly refer to the physical and chemical characteristics such as soil particle size, composition, salinity, suction, and hydraulic conductivity (An et al., 2018; Shimojimaa et al., 1996; Wilson et al., 1994). MICP has been proven to be an effective method for soil water evaporation reduction in laboratory

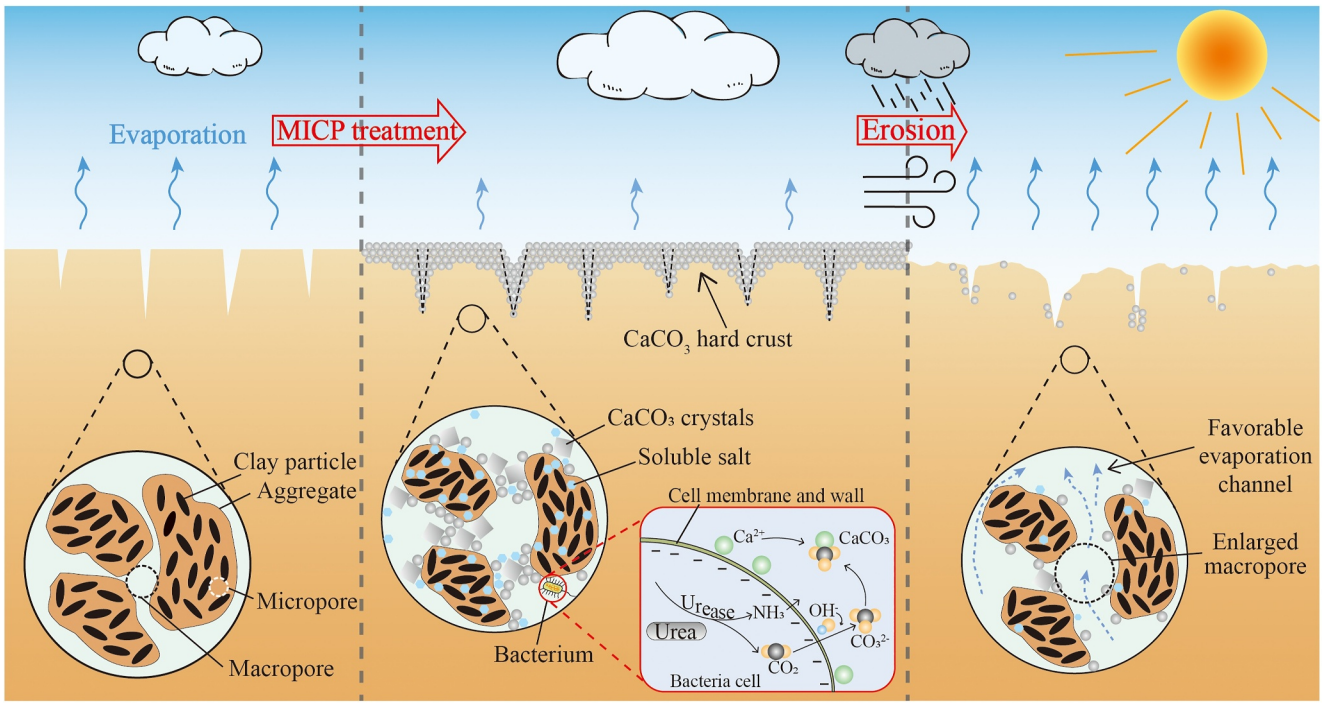

Figure 12. Schematic diagram of the process and the mechanism of long-term performance on drought mitigation through MICP method.

compacted soil (Liu et al., 2021). The reduction relies on the increase of soil suction and decline of hydraulic conductivity with the production of hard crust. However, the most distinct difference between in-situ soils and laboratory compacted soils is that in-situ soils have a loose structure with large pores (Liu, Zhu, et al., 2020), which is undoubtedly able to weaken the MICP treatment effect, and at the same time intensify the weathering and result in more rapid failure of MICP. As proven, the effect of MICP method deteriorated in the field after a long-term climate change (Figure 5). Figure 12 shows the schematic diagram of the process and the mechanism of long-term performance on drought mitigation through MICP method.

During the MICP process, the introduction of a large amount organisms and soluble salts and the generation of calcium carbonate crystals led to the change of soil pore structure and soil water retention capability, and then significantly reduced the evaporation rates of in-situ soil samples (Figure 9a). A mass of microorganisms was introduced into the in-situ clayey soil. The microbes settled at the surface of soil particles and particle-particle contacts and acted as nucleation sites (Al Qabany et al., 2012). Catalyzed by the urease produced by the microbes (DeJong et al., 2010), $CaCO_3$ crystals were precipitated which coated the soil particles and filled soil pores (Cheng et al., 2013). Furthermore, a large amount of $CaCO_3$ crystals precipitated on the soil surface, which was caused by the accumulation of BS and CS on the soil surface during the MICP treatment process due to the poor hydraulic conductivity of clayey soil (Cheng et al., 2021; Sun et al., 2023). After multiple rounds of MICP treatment, a dense hard crust was formed and covers the sample surface (as shown in Figure 4b) which played a positive role in soil water evaporation control. A similar dense surface structure can also be observed in previous studies both in MICP-cemented sand (Chu et al., 2012) and clayey soil (Cheng et al., 2021).

In addition to the generation of large quantities of $CaCO_3$ crystals, the other dramatic change in soil properties during the MICP treatment stemmed from the introduction of large amounts of soluble salts. To provide a calcium-rich environment for sufficient MICP reaction (Whiffin et al., 2007), a large amount of calcium chloride solution was added to the system. Moreover, ammonium ions produced by urea hydrolysis and various organisms such as the extracellular polymeric substances (EPS) produced by microbes, bacteria, urea, and enzymes were also deposited in the pores of the soil (He et al., 2018; Tang et al., 2020). These soluble salts and organisms in soil significantly increased the soil osmotic suction and improved the soil water retention capacity (Chen et al., 2021; Saffari et al., 2019). Consequently, the soluble salts in soil had a positive effect on the inhibition of soil evaporation process. However, the cation exchange reaction between the residual bivalent calcium ions in soil and the

monovalent metallic ions surrounding the clayey soil particles promoted the shrinkage of the soil particles' double layer and then resulted in the aggregation of soil particles (Akcanca & Aytekin, 2012; Ying et al., 2022). As shown in Figure 11b, the inter-aggregate pores expanded conspicuously and the volume of intra-aggregate pores decreased. Moreover, the soluble salt crystals filled the soil pore and further impelled the reduction of micropore density. The water retention capacity is dominated by the pore size distribution at the micro-pore range (Ying et al., 2022). Therefore, the enlarged macropores and decreased micropores in soil tended to weaken the water retention capacity of soil and had negative effects on evaporation inhabitation.

In conclusion, MICP technique performed a remarkable short-term drought mitigation capability which is attributed to the formation of hard crust and high-level osmotic suction due to the accumulation of soluble salts in soil. Soluble salts contributed to improving the soil water retention capacity. The hard crust acted as a barrier to suppress the diffusion of water vapor from soil to the atmosphere and significantly improved the evaporation resistance.

4.2. Deterioration Process of MICP Treatment Under Climate Change

The deterioration of MICP treatment suffering long-term climate change was mainly due to the loss of soluble salts and the erosion of the hard crust. As can be seen from Figures 9b and 9c, the evaporation rates of MICP-treated samples increased after washing off the soluble salts and removing the hard crust. Climatic effects include rainfall erosion, wind erosion, and slope integrity deterioration by wet-dry and freeze-thaw cycles, all of which degrade the effects of MICP treatment. As depicted in Figure 12, long-term weathering destroyed the soil surface hard crust (Cheng et al., 2021; Jiang et al., 2019) and exposed the large macropores and micro fissures formed during MICP treatment. Moreover, the soluble salt crystals and weakly cemented $CaCO_3$ crystals between soil particles were disrupted and eroded (Figure 8), carrying adjacent soil particles simultaneously, which caused expanded pores in soil. Part of macropores and micro fissures connected and generated cracks in surface soil. MIP results revealed that MICP-treated soils subjected to long-term weathering and erosion had more pronounced macropores, larger porosity, and looser soil structures (Figures 11 and 12). These macropores, micro fissures and cracks open to the atmosphere can act as advantageous channels for the escape of water vapor from the soil, thus accelerating evaporation rate (Tran et al., 2019; Zeng et al., 2023). Moreover, the enlarged soil pore size reduced the matric suction, which further resulted in weaker soil water retention capacity (Adamu & Aliyu, 2012; Germann & Beven, 1985).

From the perspective of long-term results, the effects of MICP technique on drought resistance improvement were significantly limited. Hard crust and soluble salts, the two key contributory factors, are highly susceptible to long-time weathering. In fact, regardless of hard crust and soluble salts, MICP treatment would lead to the reduction of the water retention capacity of the soil. And the evaporation rate of soil increased with the calcium carbonate precipitation. This phenomenon was predominantly attributed to the reduction of micropores and expansion of macropores which were caused by the aggregation effect of calcium ions, the filling effect of crystals on micropores, and the macropores' expansion due to crystal growth. The change of microstructure led to the reduction of water retention capacity and promoted water evaporation.

4.3. Effects of MICP Treatment Rounds and Cementation Solution Concentration on Soil Water Evaporation

MICP treatment rounds and CS concentration significantly influence the effects of MICP treatment on soil water evaporation suppression both after MICP treatment and after a long period of weathering. After MICP treatment, with an increase in MICP treatment rounds, the yield of calcium carbonate during the MICP process increased (Figure 8) and formed a denser hard crust which reduced the evaporation rate of soil. As for CS, the concentration of CS control the morphology and size of $CaCO_3$ crystals, $CaCO_3$ crystals growth rate, and $CaCO_3$ content (Lv et al., 2022; Terzis et al., 2016). In this study, higher CS concentration (1.0 M) resulted in higher $CaCO_3$ content and better performance on evaporation reduction. In addition, more MICP treatment rounds and higher CS concentration introduced more soluble salts to soil resulting in a higher osmotic suction in soil which further reduced the evaporation rate.

Soil treated with different MICP methods has various weathering resistance due to different levels of hard crust thicknesses and $CaCO_3$ content formed during MICP process, and causes different long-term drought mitigation

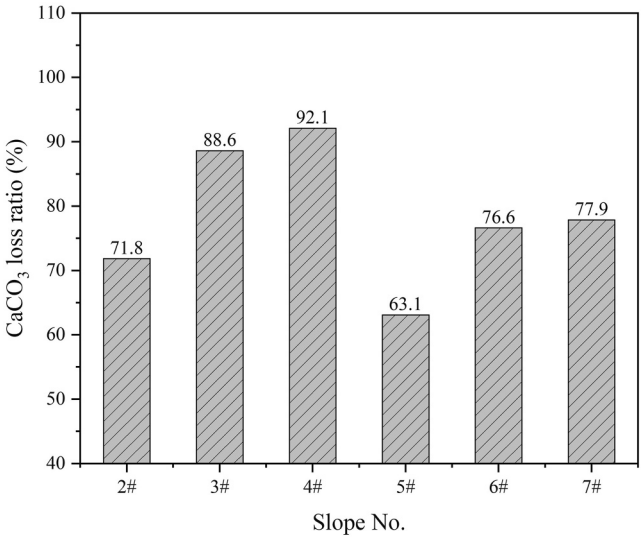

Figure 13. Calcium carbonate loss ratio (Rl) of slopes 2# to 7# after 16 months.

performance (Cheng et al., 2021; Tang et al., 2023). The $CaCO_3$ loss ratio (R_l) was defined to describe the lost MICP-induced $CaCO_3$ content during 16-month weathering and can be expressed as:

$$R_l = \frac{(C_M - C_S) - (C_R - C_S)}{C_M - C_S} \times 100\% \quad (3)$$

where C_M, C_S, and C_R are the $CaCO_3$ content of soil after MICP treatment, untreated soil, and eroded MICP-treated soil, respectively.

Figure 13 shows the calcium carbonate loss ratio (R_l) of slopes 2# to 7# after 16 months. As the MICP treatment rounds increased, the calcium carbonate loss ratio of soil increased. However, the treatment effects of soil treated by two rounds of MICP were limited because the total $CaCO_3$ yield was too low. With the increase of CS concentration, the calcium carbonate loss ratio of soil showed a decreasing trend. Consequently, the MICP treatment scheme four to six treatment rounds and 1.0 M CS had the most effective drought mitigation effect and long-term stability, though the drought mitigation effect was periodical and time-limited.

To satisfy the long-term effectiveness demand of MICP for drought mitigation of agricultural soils, regular maintenance and periodical treatments are necessary. BS and CS are required to be sprayed at certain time intervals on the target soil to repair the surface hard crust, so as to achieve the effect of suppressing evaporation. Although the soluble salts in the soil have a significant inhibitory effect on evaporation, heavy salt content is harmful to the growth of crops (Zelm et al., 2020). Therefore, the content of soluble salts is suggested to be controlled. The inhomogeneous treatment effect of MICP is also a notable issue when dealing with slopes (Figure 8a). If regular maintenance and periodical treatments are difficult to implement, measures that MICP combined with planation (Zheng et al., 2018) or biofilm can be employed as coupled phase-by-phase slope moisture retention methods. The growth of plant roots and biofilms takes a relatively long time. In the early stage, MICP measures can play a major role in soil slope drought mitigation before the vegetation root and biofilm system takes effect. After about a year or two, well-developed planation and biofilm play major roles in soil water retention, while MICP treatment degrades gradually. In addition, MICP treatment promote vegetation growth because residual urea during MICP treatment can act as nutrient (Li et al., 2020). The organic combination of these methods can improve the soil slope water retention capability in stages.

5. Conclusions

This study explores the long-term performance of drought mitigation through the bio-approach of MICP. Seven field-scale test slopes were treated with varying concentrations of cementation solutions using different MICP treatment methods and the evaporation characteristics, water retention capacity and calcium carbonate content of the test slopes were evaluated. A series of lab-scale tests for undisturbed in-situ soil samples including evaporation, suction and MIP tests were conducted after samples were subjected to MICP treatment, soluble salts washing and hard crust removal, respectively. The critical contributory factors and deterioration mechanism of MICP technique for long-term drought mitigation were revealed. Analyzing these experimental results leads to the following conclusions.

1. MICP technique can significantly suppress soil water evaporation but had a time-dependent performance on long-term drought mitigation. After 16-month weathering, MICP-induced $CaCO_3$ decreased by more than 60%. The evaporation rate of soil increased with MICP treatment rounds and concentration of CS and can reach nearly two times of untreated soil.
2. Through MICP treatment, soil evaporation rate can decrease by 50%. MICP technique exhibited a remarkable evaporation reduction capacity attributing to the soluble salts and dense hard crust. The former can improve the soil water retention capacity via increasing osmotic suction. The latter acted as a barrier suppressing the diffusion of water vapor from soil to atmosphere.

3. The deterioration of MICP treatment suffering a long-term climate change was mainly due to loss of hard crust, decreased suction and change of pore size distribution in soil. MICP treatment resulted in the connection of expanded macropores which acted as favorable evaporation channels accelerating water vapor transfer.
4. Considering MICP treatment rounds and CS concentration, the MICP treatment scheme with four to six treatment rounds and 1.0 M CS had the most effective drought mitigation effect and long-term stability. To ensure the long-term effects of MICP, periodical treatments and vegetation measures can be employed.

This study validates the time-dependent effects of MICP technique for long-term drought mitigation and provides important experience for the in-situ application of MICP technique. A further study of the regular maintenance and periodical treatments of MICP treatment is required to ensure the long-term drought resilience of MICP technique.

Data Availability Statement

All data to support this study are available on the repository: Ji et al. (2024).

Acknowledgments
This work was supported by the National Natural Science Foundation of China (Grant 41925012, 42230710), National Key Research and Development Program of China (Grant 2023YFC3707900), Key task project for joint research and development of the Yangtze River Delta Science and Technology Innovation Community (Grant 2022CSJGG1200), and Natural Science Foundation of Jiangsu Province (Grant BK20211087). The writers wish to express their gratitude to Chao Lv, Zhi-Hao Dong, Rui Wang, Ben-Gang Tian, Jin-Jian Xu, Jun-Zheng Zhang, Hui-Cong Hu, Wei-Jie Liu, Yi-Cheng Zhang, Wen Mu, Zhan-Ming Yang and Hao Liu of Nanjing University for the help to finish the sampling and tests.

References

Achal, V., Pan, X., Fu, Q., & Zhang, D. (2012). Biomineralization based remediation of As(III) contaminated soil by Sporosarcina ginsengisoli. *Journal of Hazardous Materials*, *201–202*, 178–184. https://doi.org/10.1016/j.jhazmat.2011.11.067

Adamu, G., & Aliyu, A. (2012). Determination of the influence of texture and organic matter on soil water holding capacity in and around Tomas Irrigation Scheme, Dambatta Local Government Kano State. *Research Journal of Environmental and Earth Sciences*, *4*, 1038–1044.

Akcanca, F., & Aytekin, M. (2012). Effect of wetting–drying cycles on swelling behavior of lime stabilized sand–bentonite mixtures. *Environmental Earth Sciences*, *66*(1), 67–74. https://doi.org/10.1007/s12665-011-1207-5

Al Qabany, A., Soga, K., & Santamarina, C. (2012). Factors affecting efficiency of microbially induced calcite precipitation. *Journal of Geotechnical and Geoenvironmental Engineering*, *138*(8), 992–1001. https://doi.org/10.1061/(asce)gt.1943-5606.0000666

An, N., Tang, C. S., Xu, S. K., Gong, X. P., Shi, B., & Inyang, H. I. (2018). Effects of soil characteristics on moisture evaporation. *Engineering Geology*, *239*, 126–135. https://doi.org/10.1016/j.enggeo.2018.03.028

ASTM. (2011). *Standard practice for classification of soils for engineering purposes (unified soil classification system), ASTM standard D2487*. American Society for Testing and Materials.

Chamberlain, S. D., Hemes, K. S., Eichelmann, E., Szutu, D. J., Verfaillie, J. G., & Baldocchi, D. D. (2020). Effect of drought-induced salinization on wetland methane emissions, gross ecosystem productivity, and their interactions. *Ecosystems*, *23*(3), 675–688. https://doi.org/10.1007/s10021-019-00430-5

Chen, H., Li, J., Yuan, X., Shi, B., & Shan, W. (2021). Influence of water and salt on suction characteristics of unsaturated clay: Variation, mechanism, and fitting. *Bulletin of Engineering Geology and the Environment*, *80*(11), 8535–8551. https://doi.org/10.1007/s10064-021-02435-8

Cheng, L., & Cord-Ruwisch, R. (2012). In situ soil cementation with ureolytic bacteria by surface percolation. *Ecological Engineering*, *42*, 64–72. https://doi.org/10.1016/j.ecoleng.2012.01.013

Cheng, L., Cord-Ruwisch, R., & Shahin, M. A. (2013). Cementation of sand soil by microbially induced calcite precipitation at various degrees of saturation. *Canadian Geotechnical Journal*, *50*(1), 81–90. https://doi.org/10.1139/cgj-2012-0023

Cheng, Y. J., Tang, C. S., Pan, X. H., Liu, B., Xie, Y. H., Cheng, Q., & Shi, B. (2021). Application of microbial induced carbonate precipitation for loess surface erosion control. *Engineering Geology*, *294*, 106387. https://doi.org/10.1016/j.enggeo.2021.106387

Chiang, F., Mazdiyasni, O., & AghaKouchak, A. (2021). Evidence of anthropogenic impacts on global drought frequency, duration, and intensity. *Nature Communications*, *12*(1), 2754. https://doi.org/10.1038/s41467-021-22314-w

Chu, J., Stabnikov, V., & Ivanov, V. (2012). Microbially induced calcium carbonate precipitation on surface or in the bulk of soil. *Geomicrobiology Journal*, *29*(6), 544–549. https://doi.org/10.1080/01490451.2011.592929

Cook, B. I., Ault, T. R., & Smerdon, J. E. (2015). Unprecedented 21st century drought risk in the American southwest and central plains. *Science Advances*, *1*, e1400082. https://doi.org/10.1126/sciadv.1400082

DeJong, J. T., Mortensen, B. M., Martinez, B. C., & Nelson, D. C. (2010). Bio-mediated soil improvement. *Ecological Engineering*, *36*(2), 197–210. https://doi.org/10.1016/j.ecoleng.2008.12.029

Deng, L., Peng, C., Kim, D. G., Li, J., Liu, Y., Hai, X., et al. (2021). Drought effects on soil carbon and nitrogen dynamics in global natural ecosystems. *Earth-Science Reviews*, *214*, 103501. https://doi.org/10.1016/j.earscirev.2020.103501

Fredlund, M. D., Wilson, G. W., & Fredlund, D. G. (2002). Use of the grain-size distribution for estimation of the soil-water characteristic curve. *Canadian Geotechnical Journal*, *39*(5), 1103–1117. https://doi.org/10.1139/t02-049

Germann, P. F., & Beven, K. (1985). Kinematic wave approximation to infiltration into soils with sorbing macropores. *Water Resources Research*, *21*(7), 990–996. https://doi.org/10.1029/WR021i007p00990

Gilliland, E. R. (1938). Fundamentals of drying and air conditioning. *Industrial and Engineering Chemistry*, *30*(5), 506–514. https://doi.org/10.1021/ie50341a007

He, J., Chu, J., Gao, Y., & Liu, H. (2018). Research advances and challenges in biogeotechnologies. *Geotechnical Research*, *6*(2), 144–155. https://doi.org/10.1680/jgere.18.00035

Ivanov, V., & Chu, J. (2008). Applications of microorganisms to geotechnical engineering for bioclogging and biocementation of soil in situ. *Reviews in Environmental Science and Biotechnology*, *7*(2), 139–153. https://doi.org/10.1007/s11157-007-9126-3

Ji, X. L., Tang, C. S., Pan, X. H., Cai, Z. L., Liu, B., & Wang, D. L. (2024). Long-term performance on drought mitigation through bio-approach of MICP: Evidence and insight from both field and laboratory tests[Dataset]. https://doi.org/10.5281/zenodo.10799205. *Zenodo*.

Jiang, N. J., & Soga, K. (2017). The applicability of microbially induced calcite precipitation (MICP) for internal erosion control in gravel–sand mixtures. *Géotechnique*, *67*(1), 42–55. https://doi.org/10.1680/jgeot.15.P.182

Jiang, N. J., Tang, C. S., Yin, L. Y., Xie, Y. H., & Shi, B. (2019). Applicability of microbial calcification method for sandy-slope surface erosion control. *Journal of Materials in Civil Engineering*, *31*(11). https://doi.org/10.1061/(asce)mt.1943-5533.0002897

Lai, H. J., Cui, M. J., Wu, S. F., Yang, Y., & Chu, J. (2021). Retarding effect of concentration of cementation solution on biocementation of soil. *Acta Geotechnica*, *16*(5), 1457–1472. https://doi.org/10.1007/s11440-021-01149-1

Li, C., Wang, Y., Zhou, T., Bai, S., Gao, Y., Yao, D., & Li, L. (2019). Sulfate acid corrosion mechanism of biogeomaterial based on MICP Technology. *Journal of Materials in Civil Engineering*, *31*(7), 04019097. https://doi.org/10.1061/(ASCE)MT.1943-5533.0002695

Li, L., Zhang, H., Zhou, X., Chen, M., Lu, L., & Cheng, X. (2019). Effects of super absorbent polymer on scouring resistance and water retention performance of soil for growing plants in ecological concrete. *Ecological Engineering*, *138*, 237–247. https://doi.org/10.1016/j.ecoleng.2019.07.030

Li, Q., Ye, A., Zhang, Y., & Zhou, J. (2022). The peer-to-peer type propagation from meteorological drought to soil moisture drought occurs in areas with strong land-atmosphere interaction. *Water Resources Research*, *58*(9). https://doi.org/10.1029/2022wr032846

Li, S., Li, C., Yao, D., & Wang, S. (2020). Feasibility of microbially induced carbonate precipitation and straw checkerboard barriers on desertification control and ecological restoration. *Ecological Engineering*, *152*, 105883. https://doi.org/10.1016/j.ecoleng.2020.105883

Liang, Y. L., Zhang, C. E., & Guo, D. W. (2002). Mulch types and their benefit in cropland ecosystems on the loess plateau in China. *Journal of Plant Nutrition*, *25*(5), 945–955. https://doi.org/10.1081/PLN-120003930

Liu, B., Tang, C. S., Pan, X. H., Zhu, C., Cheng, Y. J., Xu, J. J., & Shi, B. (2021). Potential drought mitigation through microbial induced calcite precipitation-MICP. *Water Resources Research*, *57*(9). https://doi.org/10.1029/2020wr029434

Liu, B., Zhu, C., Tang, C. S., Xie, Y. H., Yin, L. Y., Cheng, Q., & Shi, B. (2020). Bio-remediation of desiccation cracking in clayey soils through microbially induced calcite precipitation (MICP). *Engineering Geology*, *264*, 105389. https://doi.org/10.1016/j.enggeo.2019.105389

Liu, S., Yu, J., Peng, X., Cai, Y., & Tu, B. (2020). Preliminary study on repairing tabia cracks by using microbially induced carbonate precipitation. *Construction and Building Materials*, *248*, 118611. https://doi.org/10.1016/j.conbuildmat.2020.118611

Liu, Z., Notaro, M., & Gallimore, R. (2010). Indirect vegetation–soil moisture feedback with application to Holocene North Africa climate1. *Global Change Biology*, *16*(6), 1733–1743. https://doi.org/10.1111/j.1365-2486.2009.02087.x

Lu, Y., Gu, K., Zhang, Y., Tang, C., Shen, Z., & Shi, B. (2021). Impact of biochar on the desiccation cracking behavior of silty clay and its mechanisms. *Science of the Total Environment*, *794*, 148608. https://doi.org/10.1016/j.scitotenv.2021.148608

Lv, C., Tang, C.-S., Zhu, C., Li, W.-Q., Chen, T.-Y., Zhao, L., & Pan, X.-H. (2022). Environmental dependence of microbially induced calcium carbonate crystal precipitations: Experimental evidence and insights. *Journal of Geotechnical and Geoenvironmental Engineering*, *148*(7). https://doi.org/10.1061/(asce)gt.1943-5606.0002827

Middleton, N. (2018). Rangeland management and climate hazards in drylands: Dust storms, desertification and the overgrazing debate. *Natural Hazards*, *92*(S1), 57–70. https://doi.org/10.1007/s11069-016-2592-6

Mishra, A. K., & Singh, V. P. (2010). A review of drought concepts. *Journal of Hydrology*, *391*(1–2), 202–216. https://doi.org/10.1016/j.jhydrol.2010.07.012

Morris, P. H., Graham, J., & Williams, D. J. (1992). Cracking in drying soils. *Canadian Geotechnical Journal*, *29*(2), 263–277. https://doi.org/10.1139/t92-030

Naumann, G., Cammalleri, C., Mentaschi, L., & Feyen, L. (2021). Increased economic drought impacts in Europe with anthropogenic warming. *Nature Climate Change*, *11*(6), 485–491. https://doi.org/10.1038/s41558-021-01044-3

Okwadha, G. D. O., & Li, J. (2010). Optimum conditions for microbial carbonate precipitation. *Chemosphere*, *81*(9), 1143–1148. https://doi.org/10.1016/j.chemosphere.2010.09.066

Phillips, A. J., Lauchnor, E., Eldring, J., Esposito, R., Mitchell, A. C., Gerlach, R., et al. (2013). Potential CO2 leakage reduction through biofilm-induced calcium carbonate precipitation. *Environmental Science & Technology*, *47*(1), 142–149. https://doi.org/10.1021/es301294q

Romero, E., Della Vecchia, G., & Jommi, C. (2011). An insight into the water retention properties of compacted clayey soils. *Géotechnique*, *61*(4), 313–328. https://doi.org/10.1680/geot.2011.61.4.313

Romero, E., Gens, A., & Lloret, A. (1999). Water permeability, water retention and microstructure of unsaturated compacted Boom clay. *Engineering Geology*, *54*(1–2), 117–127. https://doi.org/10.1016/S0013-7952(99)00067-8

Saffari, R., Nikooee, E., Habibagahi, G., & van Genuchten Martinus, T. (2019). Effects of biological stabilization on the water retention properties of unsaturated soils. *Journal of Geotechnical and Geoenvironmental Engineering*, *145*(7), 04019028. https://doi.org/10.1061/(ASCE)GT.1943-5606.0002053

Samaniego, L., Thober, S., Kumar, R., Wanders, N., Rakovec, O., Pan, M., et al. (2018). Anthropogenic warming exacerbates European soil moisture droughts. *Nature Climate Change*, *8*(5), 421–426. https://doi.org/10.1038/s41558-018-0138-5

Schumacher, D. L., Keune, J., Dirmeyer, P., & Miralles, D. G. (2022). Drought self-propagation in drylands due to land–atmosphere feedbacks. *Nature Geoscience*, *15*(4), 262–268. https://doi.org/10.1038/s41561-022-00912-7

Senior, R. B. (1981). Tensile strength, tension cracks, and stability of slopes. *Soils and Foundations*, *21*(2), 1–17. https://doi.org/10.3208/sandf1972.21.2_1

Sharma, M., & Satyam, N. (2021). Strength and durability of biocemented sands: Wetting-drying cycles, ageing effects, and liquefaction resistance. *Geoderma*, *402*, 115359. https://doi.org/10.1016/j.geoderma.2021.115359

Shimojimaa, E., Yoshioka, R., & Tamagawa, I. (1996). Salinization owing to evaporation from bare-soil surfaces and its influences on the evaporation. *Journal of Hydrology*, *178*(1–4), 109–136. https://doi.org/10.1016/0022-1694(95)02826-9

Solh, M., & van Ginkel, M. (2014). Drought preparedness and drought mitigation in the developing world′s drylands. *Weather and Climate Extremes*, *3*, 62–66. https://doi.org/10.1016/j.wace.2014.03.003

Song, W.-K., & Cui, Y.-J. (2020). Modelling of water evaporation from cracked clayey soil. *Engineering Geology*, *266*, 105465. https://doi.org/10.1016/j.enggeo.2019.105465

Sun, X., Miao, L., Chen, R., Wang, H., & Wu, L. (2023). A revised porous media model of microbially induced carbonate precipitation for loess solidification. *Journal of Geotechnical and Geoenvironmental Engineering*, *149*(6). https://doi.org/10.1061/jggefk.Gteng-10309

Tang, C., Pan, X., Cheng, Y., & Ji, X. (2023). Improving hydro-mechanical behavior of loess by a bio-strategy. *Biogeotechnics*, *1*(2), 100024. https://doi.org/10.1016/j.bgtech.2023.100024

Tang, C.-S., Cui, Y.-J., Shi, B., Tang, A.-M., & Liu, C. (2011). Desiccation and cracking behaviour of clay layer from slurry state under wetting–drying cycles. *Geoderma*, *166*(1), 111–118. https://doi.org/10.1016/j.geoderma.2011.07.018

Tang, C.-S., Cui, Y.-J., Tang, A.-M., & Shi, B. (2010). Experiment evidence on the temperature dependence of desiccation cracking behavior of clayey soils. *Engineering Geology*, *114*(3–4), 261–266. https://doi.org/10.1016/j.enggeo.2010.05.003

Tang, C.-S., Shi, B., Liu, C., Gao, L., & Inyang, H. I. (2011). Experimental investigation of the desiccation cracking behavior of soil layers during drying. *Journal of Materials in Civil Engineering*, *23*(6), 873–878. https://doi.org/10.1061/(ASCE)MT.1943-5533.0000242

Tang, C.-S., Yin, L.-y., Jiang, N.-j., Zhu, C., Zeng, H., Li, H., & Shi, B. (2020). Factors affecting the performance of microbial-induced carbonate precipitation (MICP) treated soil: A review. *Environmental Earth Sciences*, *79*(5), 94. https://doi.org/10.1007/s12665-020-8840-9

Terzis, D., Bernier-Latmani, R., & Laloui, L. (2016). Fabric characteristics and mechanical response of bio-improved sand to various treatment conditions. *Géotechnique Letters*, *6*(1), 50–57. https://doi.org/10.1680/jgele.15.00134

Tran, D. K., Ralaizafisoloarivony, N., Charlier, R., Mercatoris, B., Léonard, A., Toye, D., & Degré, A. (2019). Studying the effect of desiccation cracking on the evaporation process of a Luvisol – From a small-scale experimental and numerical approach. *Soil and Tillage Research*, *193*, 142–152. https://doi.org/10.1016/j.still.2019.05.018

Vail, M., Zhu, C., Tang, C.-S., Maute, N., & Montalbo-Lomboy, M. T. (2020). Desiccation cracking behavior of clayey soils treated with biocement and bottom ash admixture during wetting–drying cycles. *Transportation Research Record: Journal of the Transportation Research Board*, *2674*(8), 441–454. https://doi.org/10.1177/0361198120924409

van Genuchten, M. T. (1980). A closed-form equation for predicting the hydraulic conductivity of unsaturated soils. *Soil Science Society of America Journal*, *44*(5), 892–898. https://doi.org/10.2136/sssaj1980.03615995004400050002x

Vicente-Serrano, S. M., Quiring, S. M., Peña-Gallardo, M., Yuan, S., & Domínguez-Castro, F. (2020). A review of environmental droughts: Increased risk under global warming? *Earth-Science Reviews*, *201*, 102953. https://doi.org/10.1016/j.earscirev.2019.102953

Whiffin, V. S., van Paassen, L. A., & Harkes, M. P. (2007). Microbial carbonate precipitation as a soil improvement technique. *Geomicrobiology Journal*, *24*(5), 417–423. https://doi.org/10.1080/01490450701436505

Wilson, G. W., Fredlund, D. G., & Barbour, S. L. (1994). Coupled soil-atmosphere modelling for soil evaporation. *Canadian Geotechnical Journal*, *31*(2), 151–161. https://doi.org/10.1139/t94-021

Xiao, Y., Zhou, W., Shi, J., Lu, H., & Zhang, Z. (2022). Erosion of biotreated field-scale slopes under rainfalls. *Journal of Performance of Constructed Facilities*, *36*(3). https://doi.org/10.1061/(asce)cf.1943-5509.0001732

Xiong, H., Peng, H., Ye, X. e., Kong, Y., Wang, N., Yang, F., et al. (2022). High salt tolerance hydrogel prepared of hydroxyethyl starch and its ability to increase soil water holding capacity and decrease water evaporation. *Soil and Tillage Research*, *222*, 105427. https://doi.org/10.1016/j.still.2022.105427

Yamanaka, T., Inoue, M., & Kaihotsu, I. (2004). Effects of gravel mulch on water vapor transfer above and below the soil surface. *Agricultural Water Management*, *67*(2), 145–155. https://doi.org/10.1016/j.agwat.2004.01.002

Yamanaka, T., Takeda, A., & Sugita, F. (1997). A modified surface-resistance approach for representing bare-soil evaporation: Wind tunnel experiments under various atmospheric conditions. *Water Resources Research*, *33*(9), 2117–2128. https://doi.org/10.1029/97WR01639

Yang, L., Yang, Y., Chen, Z., Guo, C., & Li, S. (2014). Influence of super absorbent polymer on soil water retention, seed germination and plant survivals for rocky slopes eco-engineering. *Ecological Engineering*, *62*, 27–32. https://doi.org/10.1016/j.ecoleng.2013.10.019

Yang, Y., Chu, J., Liu, H., & Cheng, L. (2022). Construction of water pond using bioslurry-induced biocementation. *Journal of Materials in Civil Engineering*, *34*(3), 06021009. https://doi.org/10.1061/(ASCE)MT.1943-5533.0004109

Ying, Z., Cui, Y.-J., Benahmed, N., & Duc, M. (2022). Changes in microstructure and water retention property of a lime-treated saline soil during curing. *Acta Geotechnica*, *17*(1), 319–326. https://doi.org/10.1007/s11440-021-01218-5

Yuan, C., Lei, T., Mao, L., Liu, H., & Wu, Y. (2009). Soil surface evaporation processes under mulches of different sized gravel. *Catena*, *78*(2), 117–121. https://doi.org/10.1016/j.catena.2009.03.002

Zelm, E. v., Zhang, Y., & Testerink, C. (2020). Salt tolerance mechanisms of plants. *Annual Review of Plant Biology*, *71*(1), 403–433. https://doi.org/10.1146/annurev-arplant-050718-100005

Zeng, Z.-J., Tang, C.-S., Cheng, Q., An, N., Chen, X.-Y., & Shi, B. (2023). A numerical model of water evaporation from cracked soil. *Computers and Geotechnics*, *162*, 105641. https://doi.org/10.1016/j.compgeo.2023.105641

Zhang, J., & Walsh, J. E. (2007). Relative impacts of vegetation coverage and leaf area index on climate change in a greener north. *Geophysical Research Letters*, *34*(15). https://doi.org/10.1029/2007GL030852

Zheng, W., Zeng, S., Bais, H., LaManna, J. M., Hussey, D. S., Jacobson, D. L., & Jin, Y. (2018). Plant growth-promoting rhizobacteria (PGPR) reduce evaporation and increase soil water retention. *Water Resources Research*, *54*(5), 3673–3687. https://doi.org/10.1029/2018WR022656